Research Article

Journal of Environmental Nanotechnology

Thermal Energy Storage Augmentation in Mini Heat Sink with Graphene Oxide/Nanodiamond Hybrid Nanofluids: Experimental and Machine Learning Approach

L. Syam Sundar*
Department of Mechanical Engineering, College of Engineering, Prince Mohammad Bin Fahd University, Al Khobar, Saudi Arabia
Received: 29.04.2025 Accepted: 21.05.2025 Published: 30.06.2025
*sslingala@gmail.com

ABSTRACT

The heat transfer coefficient, friction factor, and thermal performance factor of graphene oxide/nanodiamond (GO/ND) hybrid nanofluids flowing in a mini-heat sink were measured experimentally and validated using the ensemble machine learning. The base fluid used in this study is 60:40% (weight percentage) of water and ethylene glycol mixture, and the experiments were conducted under different volume loadings ($0 < \phi < 2\%$), and different Reynolds numbers ($1393.75 < Re < 5861.44$), respectively. Eventually, the thermophysical properties were also estimated. Results indicated that, the thermal conductivity is enhanced by 25.35% at 60 °C, and viscosity is increased by 96.60% at a temperature of 20 °C, at a volume loading of 2.0%, respectively. The Nusselt number, heat transfer coefficient, and thermal performance factor at 2.0% vol. was raised by 34.41%, 52.04%, and 1.243-times at a Reynolds number of 4181.24, with friction factor penalty of 26.82%, over the base fluid data. The XGBoost (XGB) machine learning model was used in this study. All the data of XGB predictions have shown good acceptance with the experimental values with a root-mean square errors of 1.342, 233.7763, 0.00044897, and 0.0076283, with correlation coefficients of 0.99669, 0.99257, 0.99758, and 0.98904, for Nusselt number, heat transfer coefficient, friction factor, and thermal performance factor. New Nusselt number, and friction factor correlations were also proposed.

Keywords: Heat transfer; Thermal performance factor; Graphene oxide; Nanodiamond; Machine learning.

1. INTRODUCTION

Electronic devices like personal computers, laptops need to be used within a certain temperature range to guarantee a consistent performance. It is extremely dangerous to allow the devices to exceed their maximum permitted temperature. Therefore, the cooling system needs to remove the heat from the device to maintain a constant working temperature. In the past, air cooling systems were used to cool the mini heat sink. Egan *et al.* (2008) considered a miniature heat sink with a dimension of 534 mm^2 with a profile height of 5 mm and they used air as a medium of cooling and found thermal performance improvement of 20%. Mohamed and El-Baky (2013) considered two mini channel heat-sink of rectangular shape of 5×18 mm^2, and triangular shape of 5×9 mm^2, and they found an enhanced heat transfer.

The limitations with this traditional air-cooling method is difficult to achieve an improved cooling performance. So, the air-cooling method is replaced with liquid cooling method. Peng and Peterson, (1996) used water in a microchannel to study the flow patterns and heat transmission. Heat transfer and the drop-in water pressure as it passed through a micro-channel heat sink were studied. Qu *et al.* (2022) and Makam *et al.* (2020) considered three types of mini heat-sinks like rectangular, trapezoidal and hexagonal in which water was used as a working fluid. They conducted experiments in the laminar flow ($200 < Re < 1000$) and found improved heat transfer rates. Ranjbar *et al.* (2018) analysed heat transfer for the rectangular and circular heat-sink working with water and they observed better heat transfer rates for the rectangular cross section heat-sink compared with circular channel heat-sink.

The heat transfer rates of mini-heat sink can be further improved by replacing the single-phase fluid with high thermal conductivity fluids. Choi and Jeffrey, (1995) invented the high thermal conductivity fluids called as 'nanofluids' by dispersing nanometer sized particles into the base fluid. Later, researchers have obtained an enhanced thermal conductivity compared with base fluid. Thrush *et al.* (2019) used zirconia (ZrO_2)/polyalphaolefin (PAO) base oil, Barbes *et al.* (2014) used CuO/water and ethylene glycol, while Agarwal *et al.* (2017) investigated Al_2O_3/water and ethylene glycol.

Consequently, the usage of nanofluids in mini heat-sink for improved heat transfer efficiency. Mukherjee *et al*. (2023) prepared water mixed Al_2O_3, MgO, and TiO_2 nanofluids, used in mini heat sink, and found augment of heat transfer by 24.95%, thermal resistance by 15.01% and total entropy generation by 19.96% respectively. They also noticed the better performance of Al_2O_3, MgO, and TiO_2 nanofluids. Chein and Huang, (2005) revealed improved thermal performance of Cu/water nanofluid in micro-channel heat sinks. Using a micro-channel heat sink, Lee and Mudawar (2007) investigated a water-mixed Al_2O_3 coolant and observed enhanced heat transfer characteristics. In the micro-channel heat sink, with help of water diluted Al_2O_3, and CuO nanofluids, Seyf and Mohammadian, (2011) observed thermal performance enhancement of 4.9% and 13.7%, respectively. Sheik *et al*. (2024) used SiO_2/water nanofluids in triangular mini heat sink and found thermal performance factor increase of 2.17, and 1.75 for SiO_2 nanofluid and water. Sidik (2023) observed thermal performance improvement of 6.44% and 8.33% for 2.5 vol% of water dispersed Al_2O_3, and CuO nanofluids in a divergent-convergent mini-channel heat-sink.

When water-dispersed SiO_2 was utilized in a tiny heat sink, Fazeli *et al*. (2012) found 10% less thermal resistance. The heat transfer of electronic components increased to 40% at 6.8% vol. when cooled using an Al_2O_3/water nanofluid, according to Nguyen *et al*. (2007). Selvakumar and Suresh (2012) computed a 29.63% increase in heat transfer coefficient and 15.11% increase in pumping power using experimental data of CuO/water nanofluids flowing through a heat-sink. Ho *et al*. (2021) observed improved heat transfer with water diluted nano phase change materials in a mini heat-sink. From the numerical analysis, Patel *et al*. (2024) have seen heat transfer increase of 3.05%, and Nusselt number increase of 47.8% at 5 vol% of EG20 nanofluid. Ho and Chen (2013) considered Al_2O_3/water nanofluid to replace the pure water as the coolant in a copper mini-channel heat-sink and found significantly higher average heat transfer coefficients. Saadoon *et al*. (2012) studied water based CuO, diamond, Al_2O_3, Fe_3O_4, TiO_2 and Ag nanofluids and observed that Nusselt number of Ag/water nanofluids reached to 54% at 0.075% vol. compared to other nanofluids.

The heat transfer rates of mini heat-sink can be further enhanced by using hybrid nanofluids. Before using them in a mini-sink, first it is necessary to understand the thermal conductivity of hybrid nanofluids. Sundar *et al*. (2014b) used MWCNT-Fe_3O_4/water hybrid nanofluids. Earlier we have used ND-Co_3O_4/water hybrid nanofluids and nanodiamond-Fe_3O_4 hybrid nanofluids (Sundar *et al*. 2016a). An enhanced thermal conductivity over mono nanofluids was found. Similarly, Al_2O_3-ZnO/water hybrid nanofluids (Wole-Osho *et al*. 2021), CNT-SiO_2/water hybrid nanofluids (Dalkılıc *et al*. 2018), Al_2O_3-SiO_2/water hybrid nanofluids (Yıldız *et al*. 2019; Moldoveanu *et al*. 2018) hybrid nanofluids were found to enhance thermal conductivity over the mono nanofluids. So, it is understood that, the thermal conductivity of hybrid nanofluids is higher than that of mono nanofluids.

Sriharan *et al*. (2022) used water based Al_2O_3/SiO_2, Al_2O_3/CuO, and CuO/SiO_2 hybrid nanofluids in a mini heat-sink, and observed higher heat transfer coefficient, effectiveness, and Nusselt number of 54.5%, 42%, and 28.4%, for Al_2O_3/CuO hybrid nanofluids, compared to another hybrid nanofluids. In a mini channel heat-sink with water diluted Al_2O_3 and Al_2O_3-MWCNT nanofluids, Kumar and Sarkar, (2018) studied heat transfer coefficient under the laminar flow and found maximum heat transfer coefficient improvement of 15.6% at 0.01 vol.%. without an increment of pressure drop. Baig *et al*. (2024) conducted heat transfer experiments in mini channel heat-sink with water based CuO, TiO_2, Fe_2O_3 mono nanofluids, and water based CuO-TiO_2, and CuO-Fe_2O_3 hybrid nanofluids and found 29.24%, and 24.55% enhancement of heat transfer coefficient for CuO, CuO 0.75%+Fe_2O_3 0.25% water based nanofluids, respectively, over water at a Reynolds number of 750. Heat transfer enhancement for Al_2O_3-TiO_2/water in a mini-heat sink has been observed by Kumar and Sarkar (2019). These works indicate that with the use of hybrid nanofluids, heat transfer rates can be improved mini heat sink.

From literature survey, it is found that heat transfer by reduced graphene oxide (rGO)/nanodiamond (ND) nanofluids in mini heat-sink has not been studied much. Reduced graphene oxide can be used in field effect transistors, energy storage, and composite materials, and gas sensing and high conductivity. Similarly, the nanodiamond (ND) is a good functional material, and it can be used in semiconductor, and development sectors for grinding, polishing, and surface modification of tools. If combined, rGO/ND hybrid nanoparticles might exhibit good hardness and thermal conductivity properties.

Water's freezing point (0 °C) can be increased by adding small quantities of ethylene glycol (EG). This mixture is a kind of heat transfer fluid commonly used in many energy systems to retain good heating (or cooling) ability of water, as well as broadening the operating temperature range for energy applications. In most of the cold countries like Canada, Alaska, Russia, etc., W/EG mixture can be used as car engine coolant and also for heating and ventilation applications. Practically, 60:40% W/EG is used as a heat transfer fluid. Hence in the present study, rGO/ND@60:40% (weight) hybrid nanofluids were prepared and the heat transfer, and Nusselt number phenomenon were studied while they flow in a mini heat sink. Simultaneously, 70:30% (weight) rGO/ND hybrid nanoparticles were also

investigated. Thermophysical properties were determined experimentally. The friction factor, and thermal performance factor were also estimated experimentally in the volume loadings from 0% to 2.0%, and in the turbulent flow. The obtained data were validated with XGBoost algorithm. Through the experimental data, new correlations were proposed.

2. EXPERIMENTAL STUDY

The chemicals like graphite powder, sodium nitrate ($NaNO_3$), hydrogen peroxide (H_2O_2), ethylene glycol ($C_2H_6O_2$), potassium permanganate ($KMnO_4$), hydrochloric acid (HCl), sulfuric acid (H_2SO_4), and nitric acid (HNO_3) were acquired from Sigma-Aldrich Chemicals, USA. The nanodiamond (ND) soot was obtained from International Technology Center, USA (http://www.itc-inc.org/contact.html). The distilled water is also used.

2.1 Preparation of Reduced Graphene Oxide

With help of modified Hummers (2017) approach, rGO nanoparticles were developed. About 10 g of graphite powder was dissolved in 200 ml of H_2SO_4 and 0.025 M of $NaNO_3$ and the mixture was cooled for half an hour in an ice water bath. Then, 0.039 M $KMnO_4$, was added and the mixture was shaken with an agitator for 20 minutes at 0 ℃. The solution turned into green color because of availability of oxidizing agent (permanganyl ion, MnO_3^+). The mixture was allowed to attain room temperature. The solution was treated again with 30 wt.% of H_2O_2 for around 30 minutes to remove all impurities after being thoroughly washed several times with large volumes of distilled water. Ultimately, the reduced graphene oxide (rGO) nanosheets were extracted through water using the centrifugal process. The rGO were heated at 60 ℃ for around 12 hours. During the synthesis of GO through Hummers' method the metal ions like Mn^{2+}, Fe^{3+}) and other impurities may remain. Strong acids effectively remove the impurities by forming metal chlorides, thereby purifying the surface and freeing up reactive sites for carboxylation. After graphene oxide (GO) is reduced, rGO usually has leftover oxygen functions such hydroxyl (–OH), epoxide (–O–), and carbonyl (C=O) groups. These oxygen-containing groups can be protonated by 1:3 molar ratio H_2SO_4, and HNO_3 and stir the solution with magnetic stirrer for 72 hours, which increases their reactivity and makes it easier for them to undergo subsequent hydrolysis or oxidative reactions to transform into carboxylic acid groups. The same procedure is repeated several times in order to get the large quantity of rGO nanosheets.

2.2 Purification of Nanodiamond Soot

The nanodiamond (ND)-soot was purified as follows. About 10 g of ND-soot was dispersed in 200 mL distilled water and stirred with a magnetic stirrer for 30 mins. Generally, the ND nanoparticles are synthesized through detonation technique, and which involves, TNT (trinitrotoluene) and RDX (cyclotrimethylenetrinitramine) in the weight ratio of 50:50%. Then the formed ND contain amorphous carbon and other impurities around the ND particles. Strong acid treatment is required to et pure diamond nanoparticles, for that purpose, the obtained ND-soot was treated with 1:3 molar ratio of sulfuric acid and nitric acid mixture and stir the solution for 72 hours. This process will help to removal impurities in the ND-soot and also help the formation of carboxyl groups on ND particle surface, and also helps to attach the nanoparticles on the rGO nanosheet, while they were dispersed in the base fluid. After that, distilled water was used to rinse the ND-soot several times.

2.3 Preparation of Hybrid Nanofluids and Properties

Before preparing the hybrid nanofluids, the physical properties of hybrid nanoparticles were estimated from mixture formulas. Nanoparticles of 70:30% (weight) was considered in this study. The physical properties of base fluid and nanoparticles were calculated using the equations (1)-(3).

Thermal conductivity,

$$k_{(rGO/ND)_p} = \frac{k_{rGO} \times W_{rGO} + k_{ND} \times W_{ND}}{W_{rGO} + W_{ND}} \quad \dots (1)$$

Density of particles,

$$\rho_{(rGO/ND)_p} = \frac{\rho_{rGO} \times W_{rGO} + \rho_{ND} \times W_{ND}}{W_{rGO} + W_{ND}} \quad \dots (2)$$

Specific heat,

$$C_{p_{(rGO/ND)_p}} = \frac{C_{p,rGO} \times W_{ND} + C_{p,ND} \times W_{ND}}{W_{rGO} + W_{ND}} \quad \dots (3)$$

where, k, ρ, and C_p stands for conductivity, density, and specific heat, respectively. W stands for weight.

Table 1. Properties of substances and base fluid at 20 ℃

Property	Substances			
	Base Fluid (60:40% W/EG)	ND	rGO	rGO/ND (70:30%)
ρ (kg/m^3)	1059.65	3100	1910	2267
k (W/mK)	0.404	2200	4000	3460
μ (mPa.s)	2.94	----	----	----
C_p (J/kgK)	3402	610	710	680

The hybrid nanofluids were prepared in the volume loadings of 0.5%, 1.0%, 1.5%, and 2.0%, by direct blending of hybrid particles in 60:40% W/EG fluid. Out of 10 g of hybrid particles, there are 7 and 3 g of rGO and ND particles. Similarly, the base fluid is 60:40% (weight) W/EG and through Eq. (2), the density of rGO/ND was calculated and used in Eq. (4) to get the required quantity of nanoparticles for the known volume loadings.

Volume concentration,

$$\phi = \frac{\left[\frac{W_{rGO/ND}}{\rho_{rGO/ND}}\right]}{\left[\frac{W_{rGO/ND}}{\rho_{rGO/ND}}\right]+\left[\frac{W_{basefluid}}{\rho_{basefluid}}\right]} \times 100 \quad \text{... (4)}$$

A total 10 kg of base fluid was used, in which 6 kg of water and 4 kg of ethylene glycol was used to match 60:40% (weight) of W/EG mixture, in which 86.01, 172.88, 260.64, and 349.29 g of rGO/ND nanoparticles were used to match 0.5%, 1.0%, 1.5%, and 2.0%, volume loadings, respectively.

For the preparation of 0.5% vol., 10 kg of base fluid was placed in a 30-liters drum and then added 86.01 g of hybrid nanoparticles. The mixture was vigorously stirred for 4 hours. Similarly, the other nanofluids of 1.0%, 1.5%, and 2.0% were prepared by dispersing 172.88, 260.64, and 349.29 g of rGO/ND in 10 kg of base.

If the zeta potential value is above –30 mV or +30 mV, then it can be treated as the prepared nanofluids are fully stable. With the help of Zetasizer instrument the zeta potential of each nanofluids sample was measured, and it is observed that, the zeta potential value 0.5%, 1.0%, 1.5%, and 2.0% vol. of nanofluid is –45 mV, –41 mV, –38 mV, and –36 mV, respectively. It is seen that the zeta potential values are above –30 mV (standard value), it means that the prepared hybrid nanofluids are very stable. Using the devices, experimental measurements of the fluid's characteristics, including density, viscosity, thermal conductivity, and specific heat, were made.

The thermophysical properties required for the analysis of heat transfer is not available in the open literature, hence those were estimated experimentally. Instruments like, KD-2 Pro (Decagon Devices in the USA: KS-1 sensor, length 60 mm, diameter 1.27 mm), A&D viscometer (SV-10, Japan), digital weighing machine, and differential scanning calorimeter (Mettler-Toledo, USA) were used to evaluate the properties. The parameters were computed using the equations (5)-(8).

The obtained k_{nf} of rGO/ND nanofluids raised by 5.69%, 8.66%, 10.15%, and 13.12% at 0.5%, 1.0%, 1.5%, and 2.0% vol. and at 20 ℃, against base liquid. It further raised to 12.09%, 16.74%, 22.33%, and 25.35%, respectively, at 60 ℃ (Fig. 1a). The obtained μ_{nf} of rGO/ND nanofluids raised by 56.80%, 80.61%, 88.78%, and 96.60% at 20 ℃ and at 0.5%, 1.0%, 1.5%, and 2.0% vol. against base liquid. The value further increased to 16.95%, 33.90%, 45.76%, 53.39% at 60 ℃, over the base fluid (Fig. 1b). The ρ_{nf} variation of rGO/ND nanofluid was noticed. Under 2 vol%, it is 1083.82, and 1064.15 kg/m3 at 20 ℃ and 60 ℃, under the same temperatures, the base fluid density is 1059.6, and 1039.6 kg/m^3 (Fig. 1c). The lower $C_{p,nf}$ of 3412.24 from 3454.06 J/kg K was found for 2.0% vol at 20 ℃. Likewise, lower $C_{p,nf}$ of 3543.56 from 3602 J/kg K was found for 2.0% vol at 60 ℃ (Fig. 1d).

The Prandtl number $\left(Pr = \mu/C_p k\right)$ is higher with increase of volume loadings, but Prandlt number is lower with increase of temperature. The Pr was 43.16 at 2.0% vol. of nanofluid, whereas, for base fluid, the Pr was 25.24, at 20 ℃. Similarly, the Pr for 2.0% vol. of nanofluid is 11.90, but for base fluid is 9.88 at 60 ℃. The obtained properties are provided in Table 2.

$$k_{nf} = 0.36684 + 0.001514\,T + 0.03924\,\phi \text{ ... (5)}$$

$$\mu_{nf} = 5.6724 - 0.08608\,T + 0.746\,\phi \text{ … (6)}$$

$$\rho_{nf} = 1069.987 - 0.49654\,T + 12.1722\,\phi \text{ … (7)}$$

$$C_{p,nf} = 3402.54 + 3.3165T - 28.552\,\phi \text{ … (8)}$$

20 ℃ < T < 60 ℃, and 0 < ϕ < 2.0%

Table 2. Flow properties of rGO-ND nanofluids

Property	T, (℃)	Volume concentration, ϕ (%)				
		0.0%	**0.5%**	**1%**	**1.5%**	**2.0%**
Thermal conductivity	20	0.4040	0.427	0.439	0.445	0.457
	30	0.4120	0.441	0.461	0.472	0.482
	40	0.4190	0.457	0.472	0.489	0.499
	50	0.4250	0.468	0.489	0.508	0.521
	60	0.4300	0.482	0.502	0.526	0.539

Viscosity	20	2.94	4.61	5.31	5.55	5.78
	30	2.44	3.69	4.23	4.42	4.57
	40	1.8	2.62	3.02	3.12	3.26
	50	1.3	1.79	2.01	2.09	2.16
	60	1.18	1.38	1.58	1.72	1.81
Density	20	1059.6	1065.68	1071.75	1077.79	1083.82
	30	1055.3	1061.44	1067.50	1073.56	1079.62
	40	1050.6	1056.70	1062.78	1068.86	1074.94
	50	1045.3	1051.45	1057.56	1063.67	1069.78
	60	1039.6	1045.74	1051.88	1058.02	1064.15
Specific heat	20	3468	3454.06	3440.12	3426.18	3412.24
	30	3502	3487.89	3473.78	3459.67	3445.56
	40	3535	3520.73	3506.45	3492.18	3477.9
	50	3569	3554.56	3540.11	3525.67	3511.22
	60	3602	3587.39	3572.78	3558.17	3543.56
Prandtl number	20	25.24	37.29	41.61	42.73	43.16
	30	20.74	29.18	31.87	32.40	32.67
	40	15.19	20.18	22.44	22.28	22.72
	50	10.92	13.60	14.55	14.51	14.56
	60	9.88	10.27	11.25	11.64	11.90

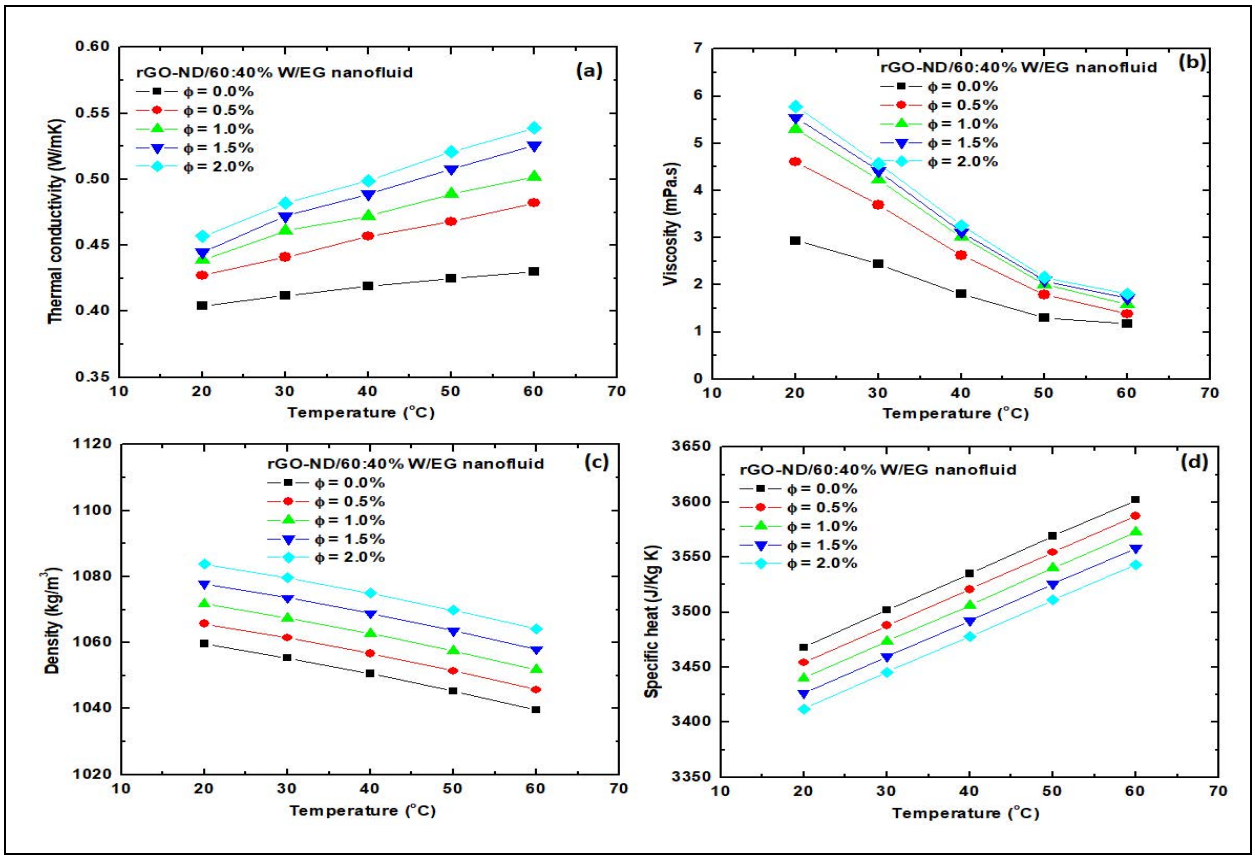


Fig. 1: Properties with respect to volume loadings, and temperatures, (a) thermal conductivity, (b) viscosity, (c) density, and (d) specific heat

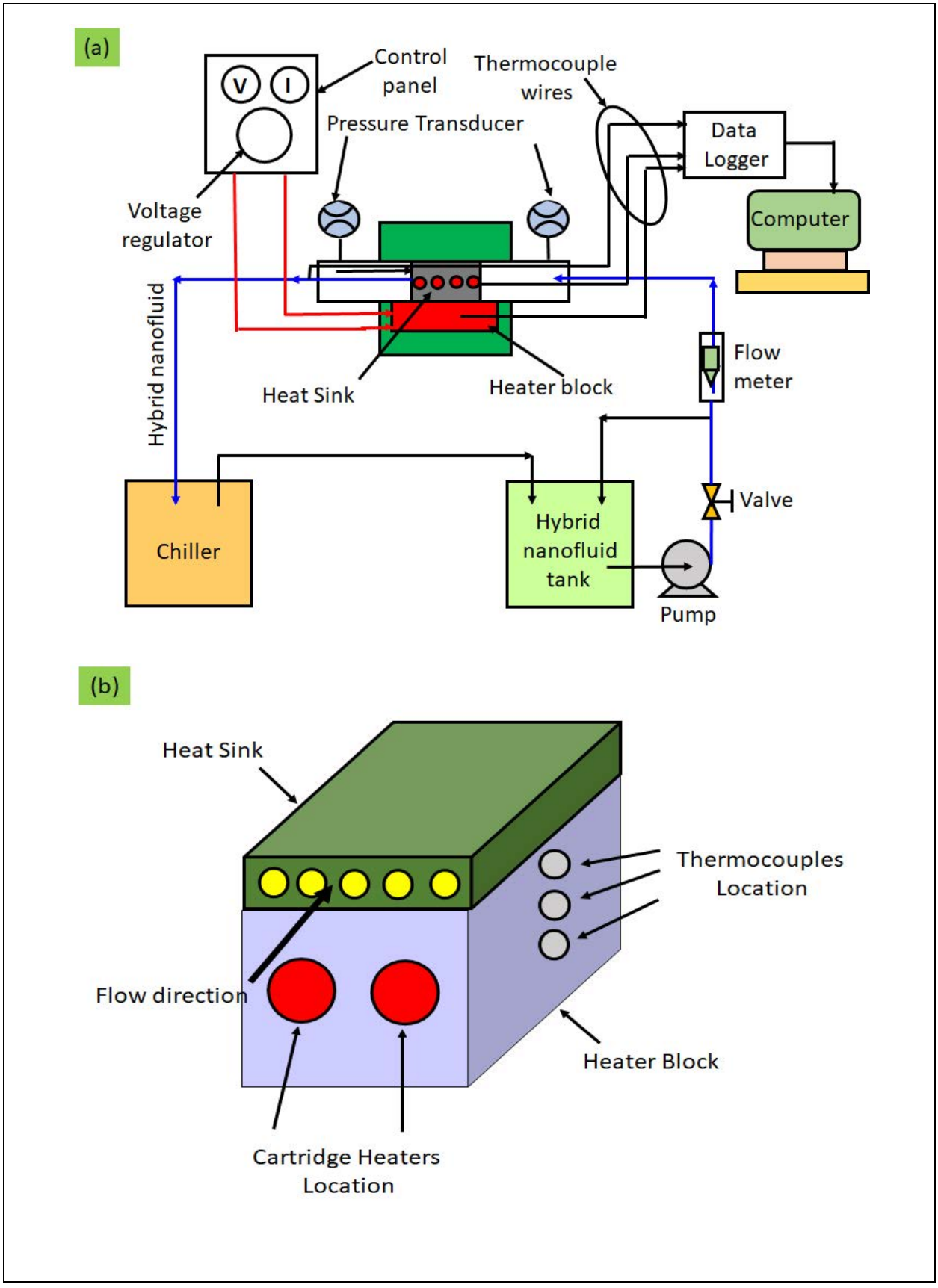


Fig. 2: (a) Line diagram of an experimental setup, and (b) test section details

2.4 Mini-heat Sink Experimental Setup

Fig. 2(a) shows the line diagram of the experimental setup. Data acquisition systems, fixed temperature water bath, and heat-sink were employed in the set up. The main component is heat sink. A square aluminium block was used to construct the heat-sink with measurements of $50 \times 50 \times 10\,mm$ $(L \times W \times H)$. Inside the block, four circular channels of 4 mm diameter were used. Four holes of 1 mm diameter with 20 mm depth were ground for fixing thermocouple next to the side wall of the heat sink's bottom surface. The thermocouples used in this experiment were all calibrated, and their accuracy was found to be ± 0.1 K. Four K-type thermocouples were put into the holes of the heat sink in order to measure the base plate temperature. Additionally, two K-type thermocouples A constant heat flux was applied at the bottom of the block.

A schematic diagram of the heater block and heat sink is shown in Fig. 2(b). To generate the heat, two heaters of 10 mm diameter were placed in the heater block. The polyurethane foam at the bottom of the heater block acts as an insulating material that restricts the from the heater block to the surroundings. To improve heat transmission efficiency, high thermal conductive grease was applied between the heat-sink and heater block. A pump allows the circulation of base fluid/hybrid nanofluid. The constant temperature bath (F10-Hc Julabo) controls the temperature of the heat-sink inlet. To keep the fluid temperature at the output consistent with the temperature at the inlet, a cooler was used. The hybrid nanofluids cool as a result of heat transfer from the reservoir's cold water. All temperatures were simultaneously monitored and recorded by connecting the thermocouples to a laptop. The manufacturer-calibrated Endress Hauser differential pressure transducer monitors drop in pressure of fluid in the heat sink with an accuracy of ± 2% and a measurement range of 0 to 250 kPa. Both sides of the heat sink included connections for the pressure transducers.

3. EXTREME GRADIENT BOOSTING (XGB)

The extreme gradient boosting (XGB) is a technique used to predict the data very accurately. Schematic illustration of the XGB model is shown in Fig. 3(a). It builds new trees progressively that aim to target the errors that are left over from the previous rounds by reducing a loss function utilizing the concept of gradient descent. Consequently, it provides enhanced efficiency and is both dependable and expandable. The obtained XGB tree of heat transfer coefficient is provided in Fig. 3(b).

Initialization:

The number of boost repetition is T

Initial value is y

The regression tree is $F_o(x) = 0$

Leaning rate is η

Training:

$t = 1$ to T is the boosting initialization

$$g_t(x) = -dL(y, F_{(t-1)}(x))/dF_{(t-1)}(x)$$

Regression tree is

$$h_t(x) = RegressionTree.Fit\big(x, -g_t(x)\big)$$

Update the predictions

$$F_t(x) = ARGMIN\{F\}\big[L\big(y, F_{t-1}(x) + \eta \times h_t(x)\big) + \Omega(F)\big] \quad \ldots (9)$$

Predictions:

The new input is x_{test}

Calculated predicted values: $x_pred = F(x_test)$

The R2, RMSE, MAE, and MSE were estimated through the below equations.

$$R^2 = 1 - \left(\frac{\sum_{i=1}^{n}(x_a - x_p)^2}{\sum_{i=1}^{n}(x_p)^2}\right) \quad \ldots (10)$$

$$RMSE = \sum_{i=1}^{n}\frac{(x_p - x_a)^2}{n} \quad \ldots (11)$$

$$MSE = \frac{1}{n}\sum_{i=1}^{n}\big(x_a - x_p\big)^2 \quad \ldots (12)$$

where n is number of points, i is observations, x_a is experimental, and x_p is XGB values.

4. RESULTS AND DISCUSSION

The rGO/ND@60:40% W/EG mixture-based hybrid nanofluids at a temperature of 20 °C was subjected to a uniform heat flux of 64000 W/m2. The top surface and side surfaces were closed with insulating material. Initially, base fluid (60:40% W/EG) was used and then hybrid nanofluids were introduced one after other. The experiments were carried out under the mass flow ($\dot{m}$) rate ranging from 1.2 to 3.6 lit/min. The Reynolds number ($Re = 4\dot{m}/\pi d\mu$) was calculated based on the mass flow and viscosity of the fluid, and it is found to be for base fluid: 1953.81 < Re < 5861.44; for 0.5% vol.: 1726.1 < Re < 5178.4; for 1.0% vol.: 1505.77 < Re < 4517.32; for 1.5% vol.: 1441.05 < Re < 4323.14; and for 2.0% vol.: 1393.75 < Re < 4181.24, respectively.

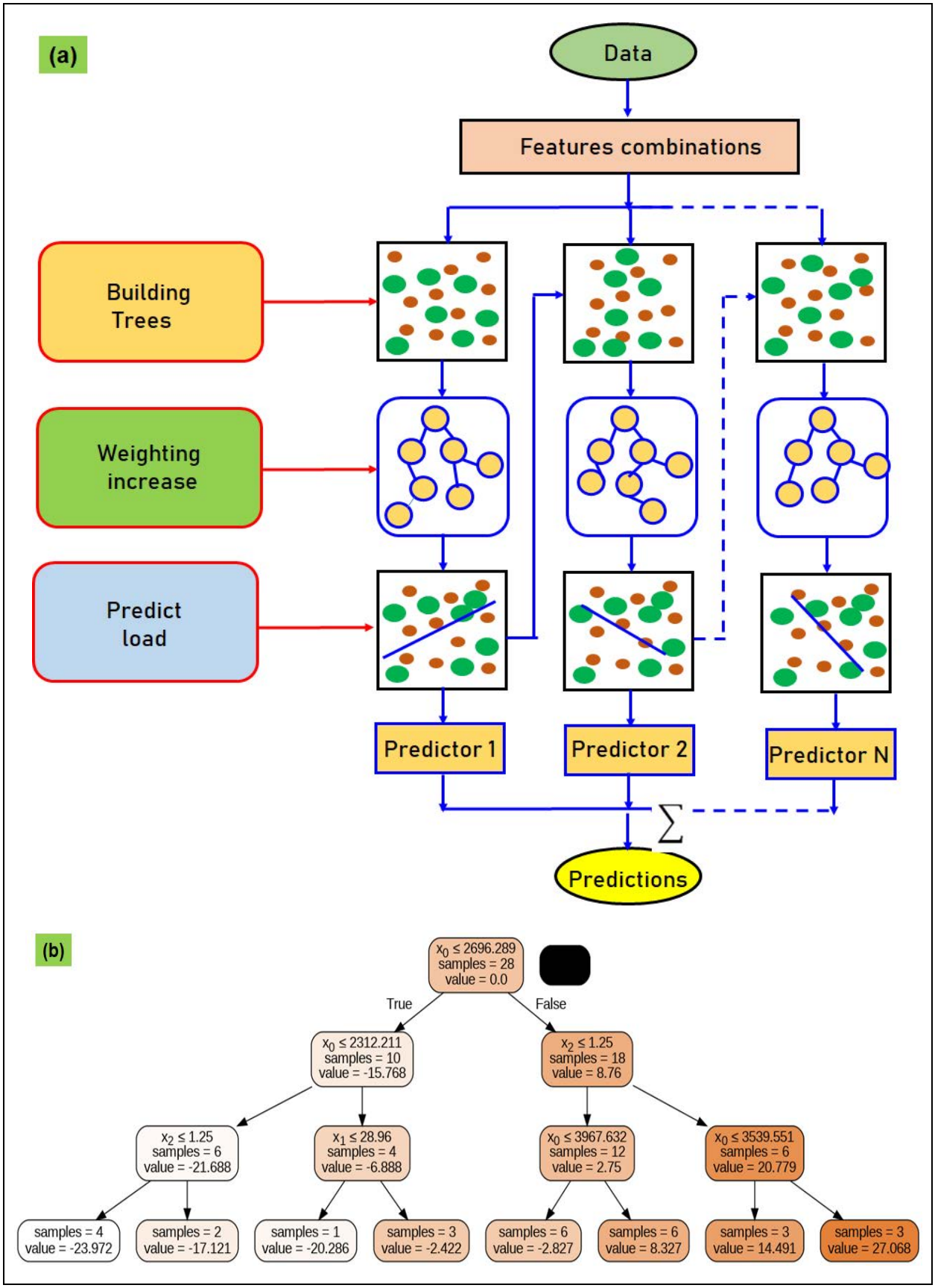


Fig. 3: (a) Schematic illustration of the XGBoost model, and (b) XGB tree for the heat transfer coefficient

4.1 Nusselt Number and Heat Transfer Coefficient

From the Eqns. (13) and (14), supplied heat, and fluid gained heat were calculated, and the difference between them was found to be ±3.2%.

Supplied heat,

$$Q_h = V.I \quad \ldots (13)$$

Fluid gained heat,

$$Q_a = \dot{m}.C_p.(T_0 - T_i) \quad \ldots (14)$$

Average heat transfer,

$$Q_{avg} = \frac{(Q_h+Q_a)}{2} \quad \ldots (15)$$

Heat transfer,

$$h_{nf} = \frac{Q_{avg}}{A(T_{wall}-T_{bulk})} \quad \ldots (16)$$

where,

$$A = \pi DL;\ T_{wall} = \frac{T_1+T_2+T_3+T_4}{4};\ T_{bulk} = \frac{T_o+T_i}{2}$$

Nusselt number,

$$Nu = \frac{h\times d}{k} \quad \ldots (17)$$

Bench-mark experiments were performed with base fluid and validated their Nusselt number through the literature method (Dittus, 1930).

$$Nu = 0.023(Re)^{0.8}(Pr)^{0.4} \quad \ldots (18)$$

Equation (17) gives the experimental Nusselt number and the Eq. (18) gives the Dittus-Boelter Nusselt number and between these two, a maximum deviation of ± 4.25% was observed.

From Eq. (17), Nusselt number of the hybrid nanofluid was estimated (Fig. 4(a)). The Nu is higher when ϕ and Re is higher. A higher Nu by 6.43%, 10.72%, 16%, and 18.14% at 0.5%, 1.0%, 1.5%, and 2.0% vol. of nanofluids at Re of 1726.1, 1505.77, 1441.05, and 1393.75 were seen against base fluid. Apparently, increased Nu by 14.17%, 18.12%, 26.14%, and 34.41% at 0.5%, 1.0%, 1.5%, and 2.0% vol. of hybrid nanofluids at Re of 5178.4, 4517.32, 4323.14, and 4181.24 were seen when validated with base fluid. Larger Nu was noticed due to the larger k_{nf}.

We have already reported hybrid nanofluids of water mixed MWCNT-Fe_3O_4 and observed a 31% rise in Nusselt number at 0.3% vol. under a Reynolds number of 22,000 (Sundar *et al*. 2004).

It is evident from the current study on rGO/ND hybrid nanofluids that the Nusselt number increases as the Reynolds number and the concentration of nanoparticles rise. This is because, in comparison to the base fluid, the suspended nanoparticles in the hybrid nanofluids have a higher conductivity. The thermophysical characteristics of the nanoparticles and the Brownian motion of the particles are also responsible for the Nusselt number enhancement for the rGO-ND nanofluid. In the current work, thermophysical properties were measured experimentally. It was shown that improved thermophysical qualities resulted in an increased heat transfer coefficient when particle volume loadings increased.

Heat transfer coefficient (h_{nf}) was obtained from Eq. (15) (Fig. 4(b)). The h_{nf} is increased by 12.49%, 20.32%, 27.77%, and 33.64% at 0.5%, 1.0%, 1.5%, and 2.0% vol. of nanofluids at Re of 1726.1, 1505.77, 1441.05, and 1393.75, against base fluid. The h_{nf} is higher by 20.67%, 28.35%, 38.94%, and 52.04% at 0.5%, 1.0%, 1.5%, and 2.0% of hybrid nanofluids at Re of 5178.4, 4517.32, 4323.14, and 4181.24, when validated with base fluid.

4.2 Friction Factor

Friction factor,

$$f = \frac{\Delta P}{\left(\frac{L}{d_i}\right)\left(\frac{\rho v^2}{2}\right)} \quad \ldots (19)$$

The f from Eq. (19) and Eq. (20) deviates ± 4.69%.

$$f = 0.3164Re^{-0.25} \quad \ldots (20)$$

(Blasius, 1908)

Equation (19) gives f of nanofluids and it was increased by 6.45%, 13.67%, 19.08%, and 24.49% at 0.5%, 1.0%, 1.5%, and 2.0% vol. of nanofluids at Re of 1726.1, 1505.77, 1441.05, 1393.75, against base fluid (Fig. 4c). The f is higher by 8.03%, 15.08%, 22.13%, and 26.82% at 0.5%, 1.0%, 1.5%, and 2.0% of hybrid nanofluids at Re of 5178.4, 4517.32, 4323.14, and 4181.24, over base fluid.

4.3 Thermal Performance Factor

Thermal performance factor was calculated as

$$TPF = \frac{\left(\frac{Nu_{nf}}{Nu_{bf}}\right)}{\left(\frac{f_{nf}}{f_{bf}}\right)^{1/3}} \quad \ldots (21)$$

The TPF values are shown in Fig. 4(d). The TPF is increased by 1.043, 1.061, 1.095, and 1.099-times at 0.5%, 1.0%, 1.5%, and 2.0% vol. of nanofluids at Re of

1726.1, 1505.77, 1441.05, and 1393.75, over base fluid. TPF is higher by 1.113, 1.128, 1.181, and 1.243-times at 0.5%, 1.0%, 1.5%, and 2.0% of hybrid nanofluids at *Re* of 5178.4, 4517.32, 4323.14, and 4181.24, when validated with base fluid. The data used for machine learning analysis is provided in Table 3.

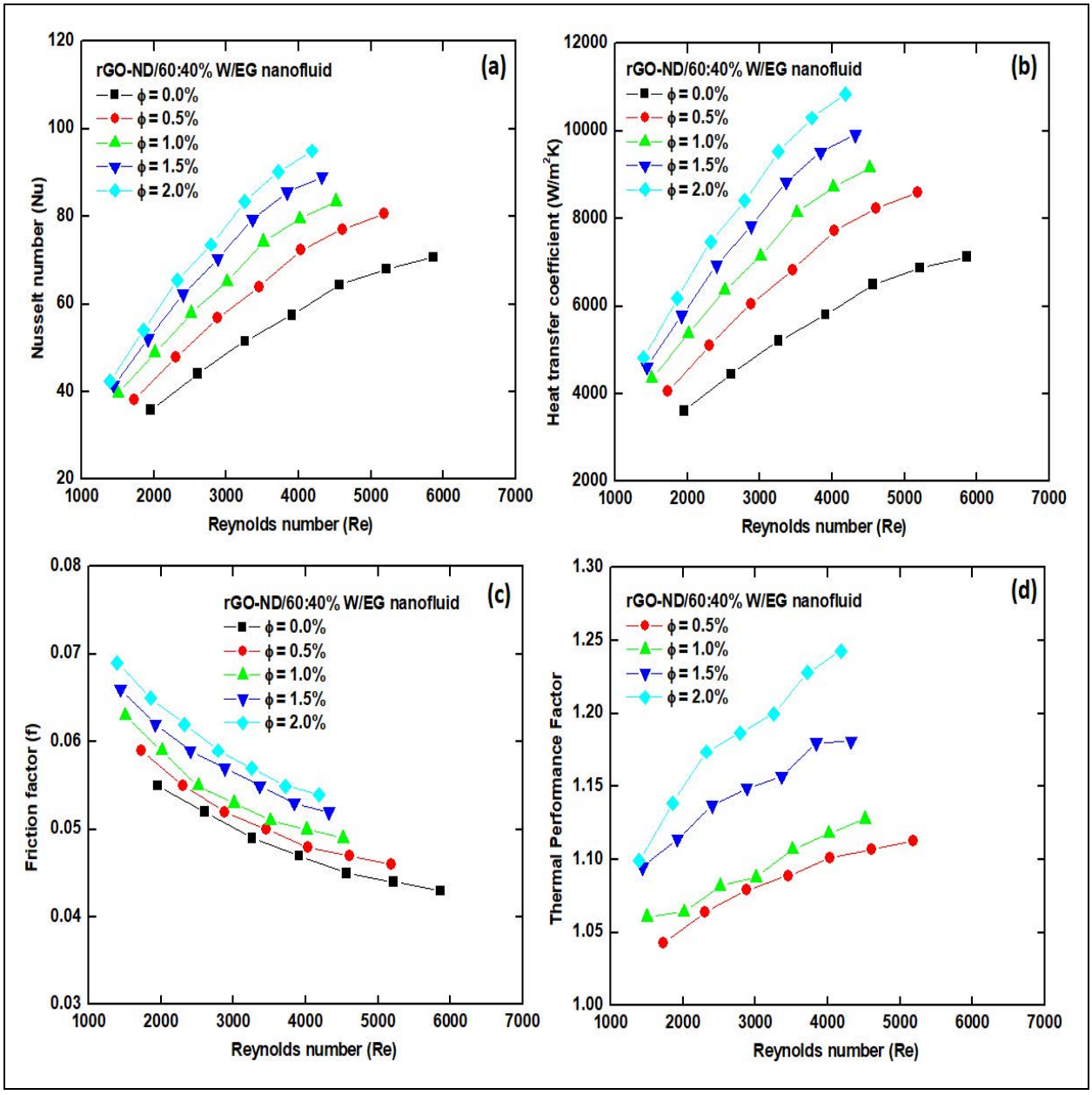


Fig. 4: Experimental data of rGO/ND nanofluids: (a) Nusselt number, (b) heat trasfer coefficeint, (c) friction factor, and (d) thermal performance factor

4.4 XGB Results

4.4.1 Nusselt Number

A total of 35 data points of Nusselt number were used for XGB model, of which 28 were considered for training, and 7 for testing the values. From the model, R2, MSE, and RMSE were analysed, and their outcomes are indicated in Fig. 5(a-i). The experimental *Nu* data and the XGB *Nu* were almost matching with each other. In the case of training data, the MSE is 0.004797, and RMSE is 0.06926. Similarly, in the case of test data, the MSE is 8.9859, and RMSE is 2.9977. In the case of all data, the MSE is 1.801, and RMSE is 1.342. The R2 values for training data is 0.9999, for test data is 0.98563, and for all data is 0.99669.

Table 3. The data used for ML analysis

S. No.	Input		Output			
	Reynolds Number	ϕ, (%)	Nusselt Number	Heat Transfer Coefficient	Friction Factor	Thermal Performance Factor
1	1953.81	0	35.85	3620.46	0.0554	---
2	2605.08	0	44.07	4451.02	0.0517	---
3	3256.35	0	51.60	5211.38	0.0490	---
4	3907.62	0	57.52	5809.13	0.0469	---
5	4558.89	0	64.41	6505.61	0.0452	---
6	5210.17	0	68.08	6876.07	0.0438	---
7	5861.44	0	70.67	7137.27	0.0426	---
8	1726.13	0.5	38.15	4072.51	0.059	1.042
9	2301.51	0.5	47.85	5107.99	0.055	1.064
10	2876.89	0.5	56.78	6061.27	0.052	1.079
11	3452.26	0.5	63.98	6829.87	0.050	1.089
12	4027.64	0.5	72.35	7723.36	0.048	1.101
13	4603.02	0.5	77.12	8232.56	0.047	1.106
14	5178.40	0.5	80.68	8612.59	0.046	1.113
15	1505.77	1	39.69	4355.98	0.063	1.061
16	2007.70	1	48.98	5375.56	0.059	1.064
17	2509.62	1	57.98	6363.31	0.055	1.081
18	3011.55	1	65.12	7146.92	0.053	1.087
19	3513.47	1	74.18	8141.26	0.051	1.106
20	4015.40	1	79.48	8722.93	0.050	1.117
21	4517.32	1	83.47	9160.83	0.049	1.127
22	1441.05	1.5	41.58	4625.78	0.066	1.095
23	1921.40	1.5	52.12	5798.35	0.062	1.114
24	2401.74	1.5	62.37	6938.66	0.059	1.137
25	2882.09	1.5	70.48	7840.90	0.057	1.149
26	3362.44	1.5	79.48	8842.15	0.055	1.156
27	3842.79	1.5	85.57	9519.66	0.053	1.180
28	4323.14	1.5	89.14	9916.83	0.052	1.180
29	1393.75	2	42.35	4838.49	0.069	1.099
30	1858.33	2	54.12	6183.21	0.065	1.1389
31	2322.91	2	65.45	7477.66	0.062	1.173
32	2787.50	2	73.65	8414.51	0.059	1.187
33	3252.08	2	83.41	9529.59	0.057	1.199
34	3716.66	2	90.15	10299.64	0.055	1.228
35	4181.24	2	94.98	10851.47	0.054	1.242

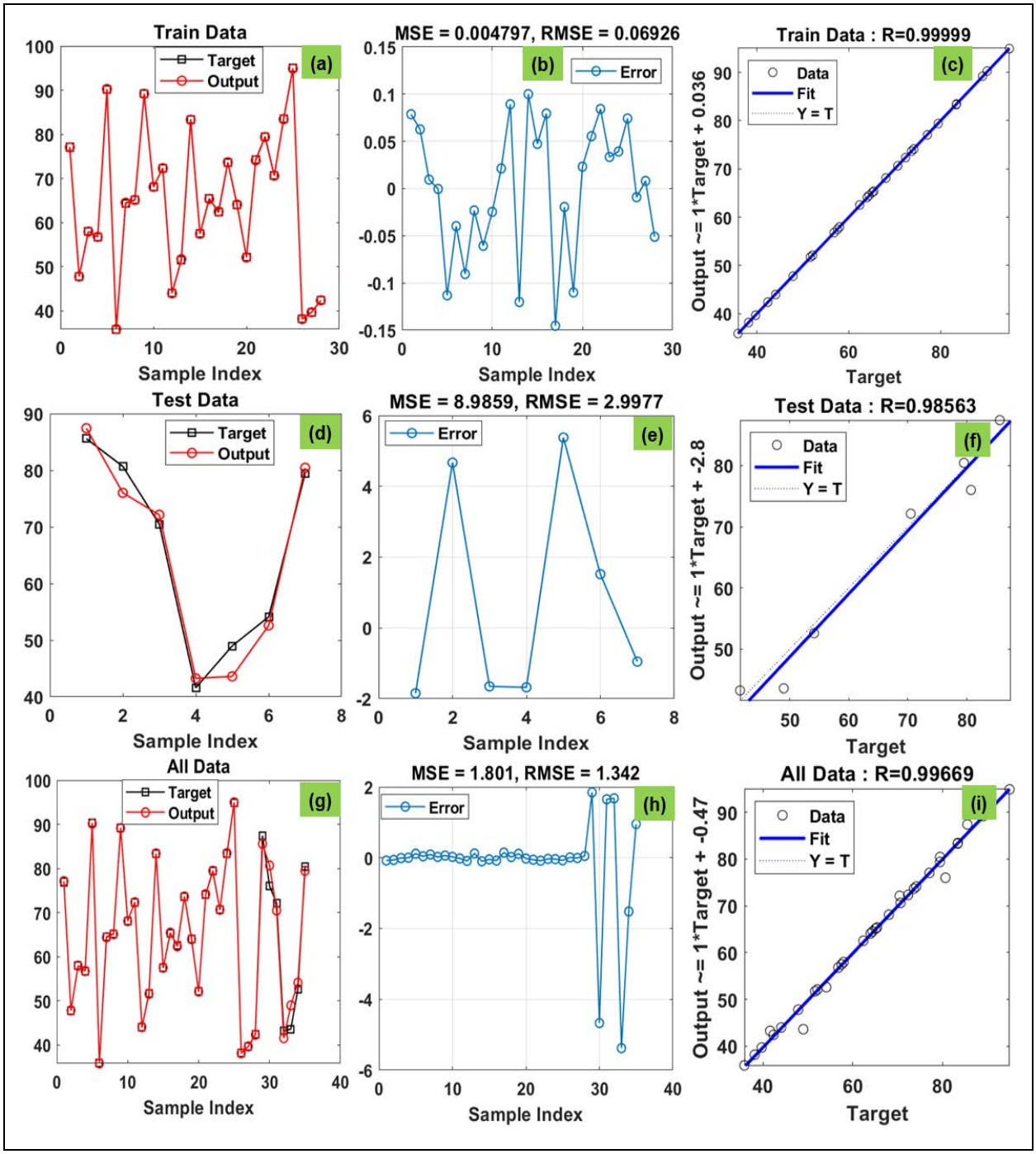


Fig. 5: XGB predictions of Nusselt number of rGO/ND nanofluids

4.4.2 Heat Transfer Coefficient

A of total 35 data points of heat transfer coefficient was used for XGB model as earlier. From model, R2, MSE, and RMSE were analysed, and their outcomes are shown in Fig. 6(a-i). The experimental h_{nf} and the XGB h_{nf} is almost matching with each other. In the case of training data, the MSE is 161.7427, and RMSE is 12.717. In the case of test data, the MSE is 264802.59, and RMSE is 514.589. Similarly, for all data, the MSE is 54641.35, and RMSE is 233.7763. The R2 values for training data is 0.9998, test data is 0.96036, and all data is 0.99257.

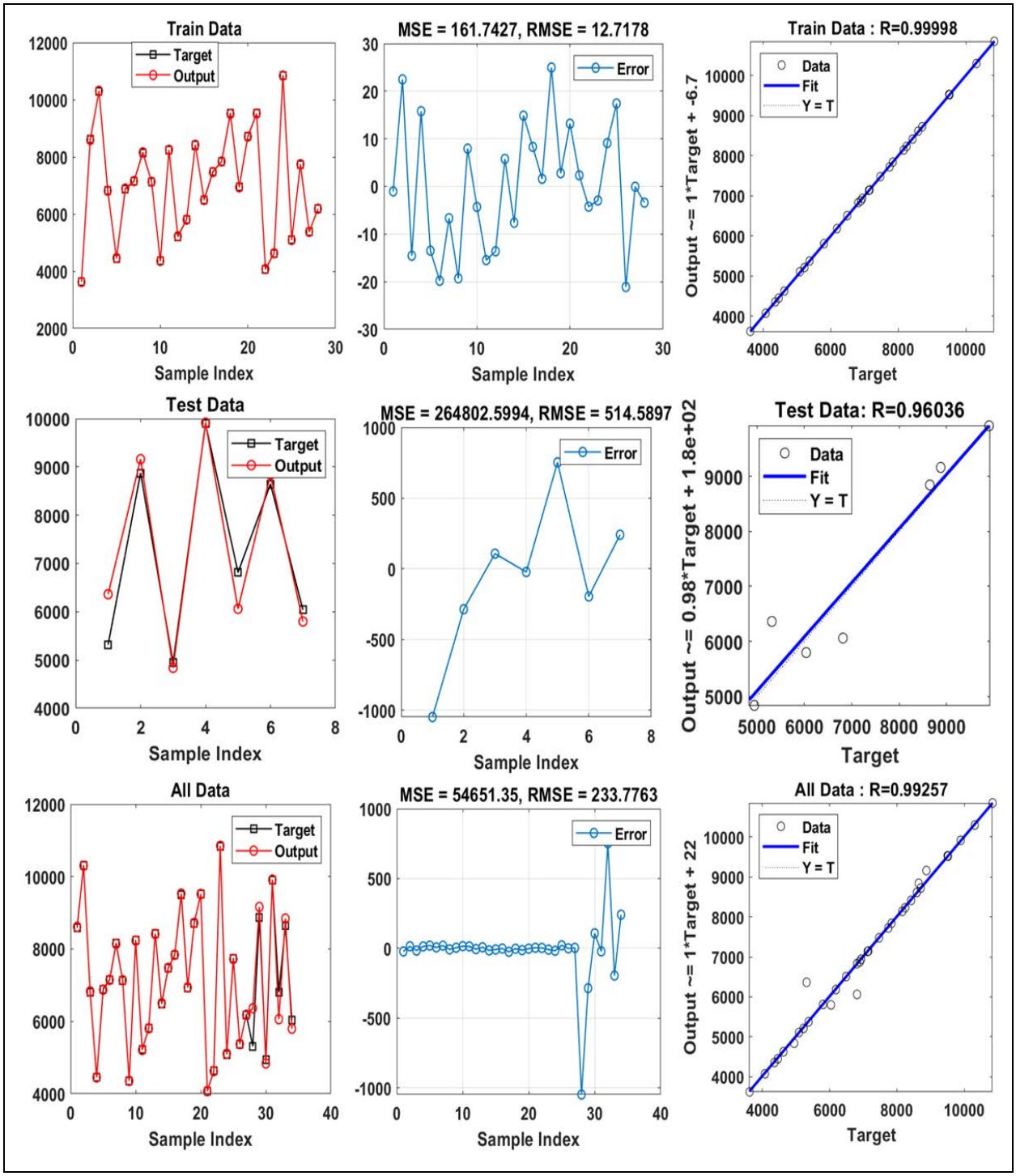


Fig. 6: XGB predictions of heat transfer coefficient of rGO/ND nanofluids

4.4.3 Friction Factor

A total of 35 data points of friction factor was used for XGB model as earlier. From the model, R2, MSE, and RMSE were analysed, and their values are provided in Fig. 7(a-f). The experimental friction factor, and the XGB friction factor data is almost matching with each other. In the case of training data, the MSE is 2.8618e-10, and RMSE is 1.6917e-05. In the case of test data, the MSE is 1.0067e-06, and RMSE is 0.0010034. In the case of all data, the MSE is 2.0158e-07, and RMSE is 0.00044897. The R2 values for training data is 1, test data is 0.99006, and all data is 0.99758.

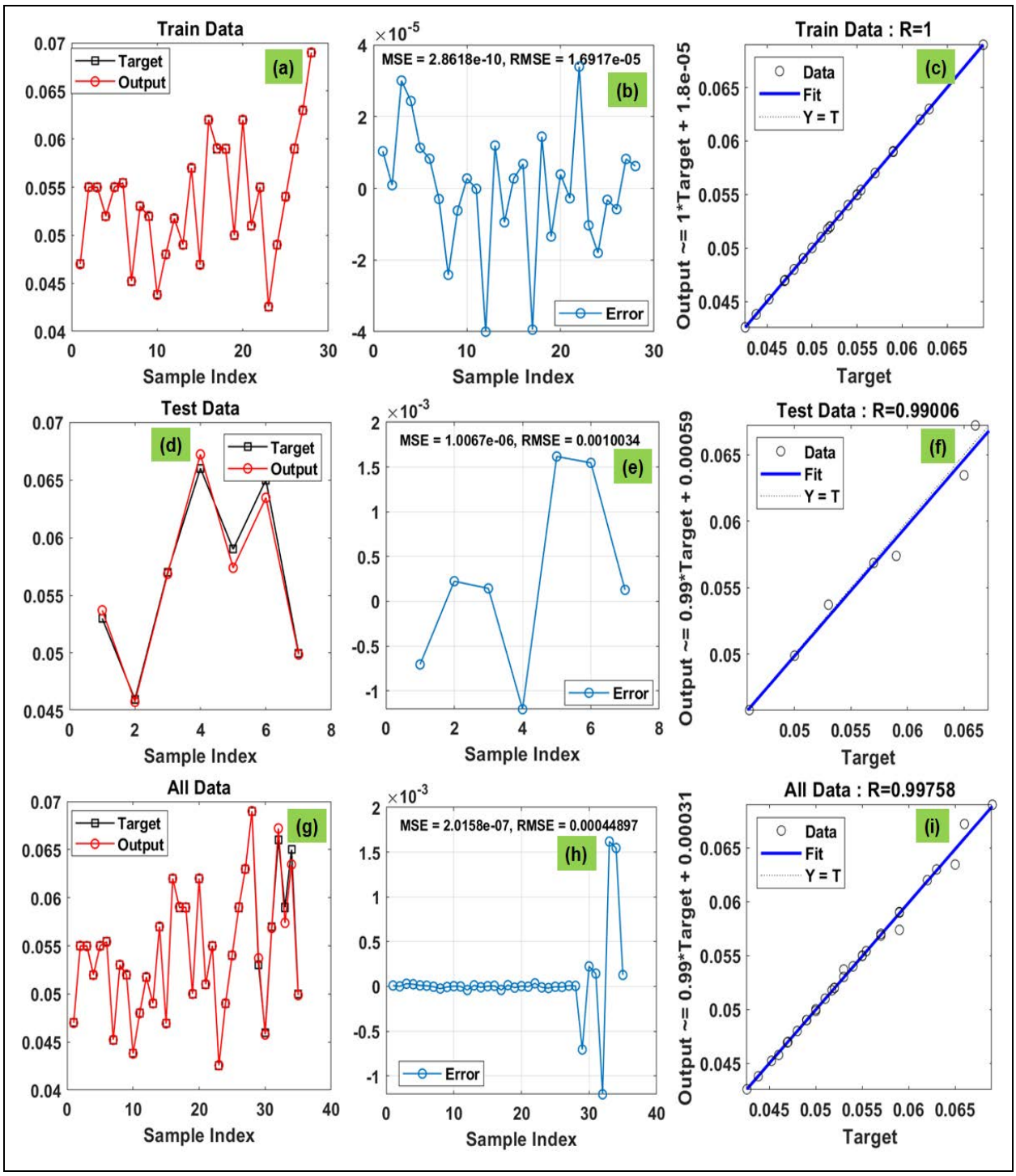


Fig. 7: XGB predictions of friction factor of rGO/ND nanofluids

4.4.4 Thermal Performance Factor

A total of 28 data points of TPF were used for XGB model, of which 23 were utilized for training and 5 for testing. From the model, the R2, MSE, and RMSE were analysed (Fig. 8(a-f)). The experimental TPF and the XGB TPF is almost matching with each other. In the case of training data, the MSE is 3.521e-5, and RMSE is 0.00018764. In the case of test data, the MSE is 0.00027143, and RMSE is 0.016475. In the case of all data, the MSE is 5.8191e-05, and RMSE is 0.0076283. The R2 values for training data is 0.9999, test data is 0.95041, and all data is 0.98904.

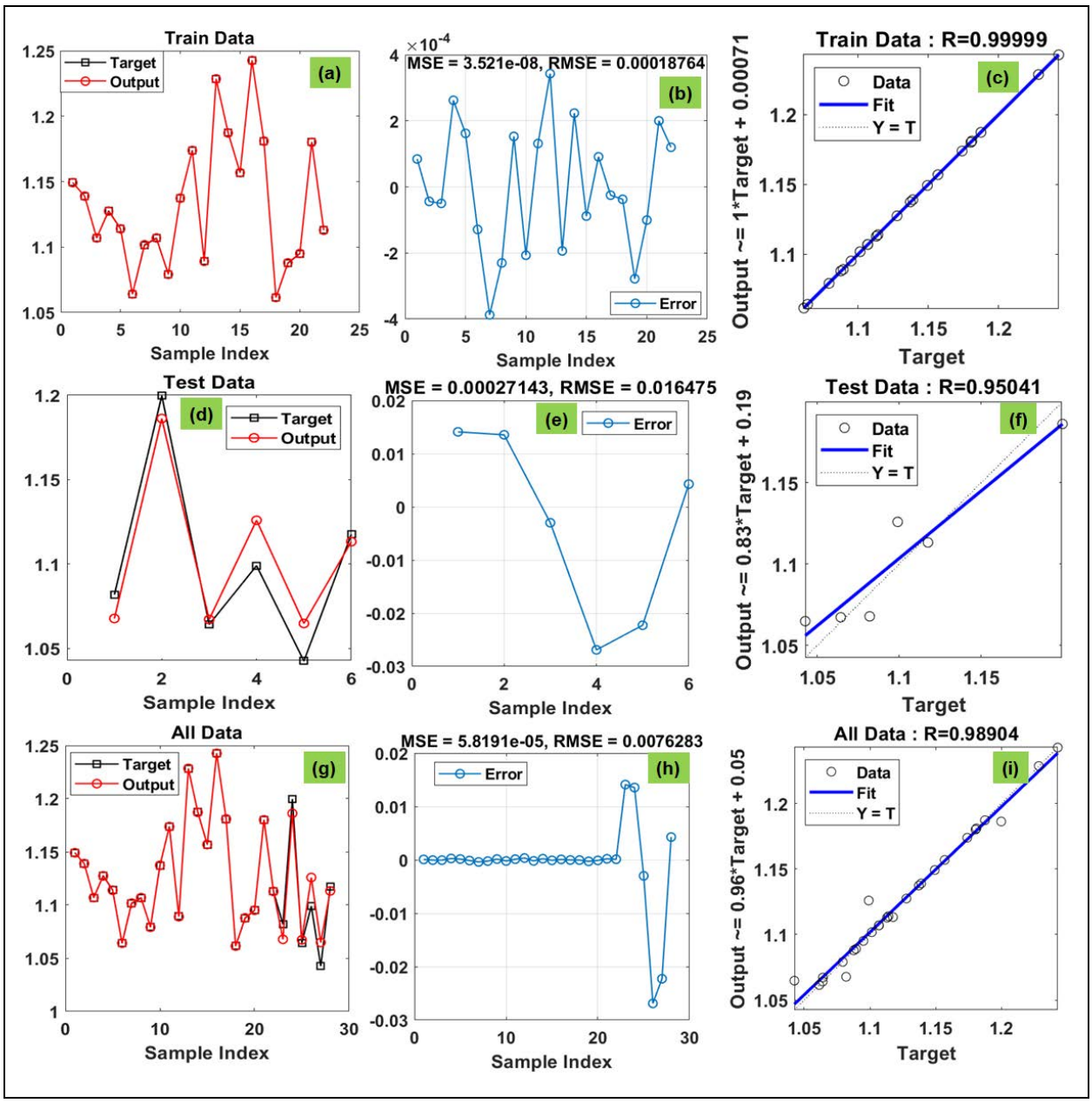


Fig. 8: XGB predictions of TPF of rGO/ND nanofluids

4.5 Proposed Correlations

Mohamed and El-Baky, (2013) equation:

$$Nu = 0.052\, Re^{0.6} Pr^{0.3} \sqrt{H/w} \quad \ldots (22)$$

Validity: 3×103 < Re < 5×104

Through the experimental data, the new correlations were developed.

$$Nu = 6.62649 + 0.013362Re + 15.1578\phi \ \ldots (23)$$

$$f = 0.06323 - 0.0000040653Re + 0.00399495\phi \quad \ldots (24)$$

$$TPF = 0.934 + 0.000029Re + 0.08085\phi \quad \ldots (25)$$

5. CONCLUSIONS

In order to cool the heat generated devices like processors in the computers, mini-heat sink concept is used. In this study, a mini-heat sink was experimentally evaluated using stable 60:40 W/EG-based rGO/ND hybrid nanofluids under varying concentrations and flow rates. The thermophysical properties of the nanofluids showed significant improvements in thermal conductivity and viscosity compared to the base fluid. At higher concentrations, enhancements were observed in Nusselt number, heat transfer coefficient, and thermal performance factor, indicating superior thermal

performance. Although friction factor increased, the overall heat transfer benefits outweighed the penalty. Machine learning analysis using XGBoost validated the experimental results with high accuracy and low deviation, confirming the reliability of the data and the effectiveness of hybrid nanofluids in enhancing mini-heat sink performance.

APPENDIX - A: UNCERTAINTY ANALYSIS

With help of a reported work (Beckwith *et al*. 1990), the uncertainties in the process calculation was analysed, and their data is given in Table 4.

$$\delta h = \sqrt{\left(\frac{\partial h}{\partial Q}\delta Q\right)^2 + \left(\frac{\partial h}{\partial T_s}\delta T_s\right)^2 + \left(\frac{\partial h}{\partial T_m}\delta T_m\right)^2} \quad \ldots (a1)$$

Then,

$$\frac{\delta h}{h} = \sqrt{\left(\frac{\delta Q}{Q}\right)^2 + \left(\frac{\delta T_s}{T_s - T_m}\right)^2 + \left(\frac{\delta T_m}{T_s - T_m}\right)^2} \quad \ldots (a2)$$

$$\frac{\delta Q}{Q} = \sqrt{\left(\frac{\delta k}{k}\right)^2 + \left(\frac{\delta T_o}{T_i - T_m}\right)^2 + \left(\frac{\delta T_i}{T_s - T_m}\right)^2 + \left(\frac{\delta D}{D}\right)^2} \quad \ldots (a3)$$

Table 4. Uncertainty values

Quantity	Uncertainty
ΔT, (oC)	0.1536
Δk, (W/mK)	0.0522
ΔL, (m)	4.25 x 10-5

FUNDING

This research received no specific grant from any funding agency in the public, commercial, or not-for-profit sectors.

CONFLICTS OF INTEREST

The authors declare that there is no conflict of interest.

COPYRIGHT

This article is an open-access article distributed under the terms and conditions of the Creative Commons Attribution (CC BY) license (http://creativecommons.org/licenses/by/4.0/).

REFERENCE

Agarwal, R., Verma, K., Agrawal, N. K. and Singh, R., Sensitivity of thermal conductivity for Al_2O_3 nanofluids, *Exp. Therm. Fluid. Sci.*, 80, 19–26(2017). https://doi.org/10.1016/j.expthermflusci.2016.08.007

Baig, T., Tariq, H. A., Anwar, M., Shoukat, A. A., Ali, H. M. and Janjua, M. M., Hydrothermal performance of mini-channel heat sink using nanofluids/hybrid nanofluids: A numerical study, *Energy Sources Part A*, 46(1), 4628–4646(2024). https://doi.org/10.1080/15567036.2024.2323155

Barbes, B., Paramo, R. and Blanco, E. Carlos, C., Thermal conductivity and specific heat capacity measurements of CuO nanofluids, *J. Therm. Anal. Calorim.*, 115(2), 1883–1891(2014). https://doi.org/10.1007/s10973-013-3518-0

Beckwith, T. G., Marangoni, R. D. and Lienhard, J. H., Mechanical Measurements, 5th Ed., *Addison–Wesley Publishing Company, New York*., 45–112(1990).

Blasius, H., Grenzschichten in Flussigkeiten mit kleiner Reibung (German), *Zeitschrift für angewandte Mathematik und Physik*, 56, 1–37(1908).

Chein, R. and Huang, G., Analysis of microchannel heat sink performance using nanofluids, A*ppl. Therm. Eng.*, 25(17-18), 3104–3114(2005). https://doi.org/10.1016/j.applthermaleng.2005.03.008

Choi, S. U. S. and Jeffrey, A. E., Enhancing thermal conductivity of fluids with nanoparticles, *ASME FED-66*, 231(66), 99–103 (1995).

Dalkılıc, A. S., Yalcin, G., Kucukyıldırım, B. O., Oztuna, S., Eker, A. A., Jumpholkul, C., Nakkaew, S. and Wongwises, S., Experimental study on the thermal conductivity of water-based CNT-SiO_2 hybrid nanofluids, *Int. Comm. Heat. Mass. Transfer.*, 99, 18–25(2018). https://doi.org/10.1016/j.icheatmasstransfer.2018.10.002

Dittus, F. W. and Boelter, L. M. K., Heat transfer in automobile radiators of the tubular type, *Univ. Calif. Publ. Eng.*, 11(2), 443–461(1930).

Egan, V., Stafford, J., Walsh, P., Walsh, E. and Grimes, R., An experimental study on the performance of miniature heat sinks for forced convection air cooling, *11th Intersociety Conference on Thermal and Thermomechanical Phenomena in Electronic Systems, Orlando, FL, USA*, 497–509 (2008). https://doi.org/10.1109/itherm.2008.4544310

Fazeli, S. A., Hashemi, S. M. H., Zirakzadeh, H. and Ashjaee, M., Experimental and numerical investigation of heat transfer, in a miniature heat sink utilizing silica nanofluid, *Superlattices. Microstruct.*, 51(2), 247–264(2012). https://doi.org/10.1016/j.spmi.2011.11.017

Ho, C. J., Hsu, S. T., Yang, T. F., Chen, B. L., Rashidi, S. and Yan, W. M., Cooling performance of mini-channel heat sink with water-based nano-PCM emulsion-An experimental study, *Int. J. Therm. Sci.*, 164, 106903(2021). https://doi.org/10.1016/j.ijthermalsci.2021.106903

Ho, C. J. and Chen, W. C., An experimental study on thermal performance of Al_2O_3/water nanofluid in a minichannel heat sink, *Appl. Therm. Eng.*, 50(1), 516–522(2013). https://doi.org/10.1016/j.applthermaleng.2012.07.037

Kumar, V. and Sarkar, J., Numerical and experimental investigations on heat transfer and pressure drop characteristics of Al_2O_3-TiO_2 hybrid nanofluid in minichannel heat sink with different mixture ratio, *Powder. Technol.*, 345, 717–727 (2019). https://doi.org/10.1016/j.powtec.2019.01.061

Kumar, V. and Sarkar, J., Two-phase numerical simulation of hybrid nanofluid heat transfer in minichannel heat sink and experimental validation, *Int. Commun. Heat, Mass. Transfer.*, 91, 239–247(2018). https://doi.org/10.1016/j.icheatmasstransfer.2017.12.019

Lee, J. and Mudawar, I., Assessment of the effectiveness of nanofluids for single-phase and two-phase heat transfer in micro-channels, *Int. J. Heat. Mass. Transfer.*, 50(3-4), 452–463(2007). https://doi.org/10.1016/j.ijheatmasstransfer.2006.08.001

Makam, J. S. and Totla, N. B., Heat transfer characteristics of water cooled minichannel heat sink using different fluid flow geometries, *IOP. Conf. Ser. Mater. Sci. Eng.*, 998(1), 012018(2020). https://doi.org/10.1088/1757-899x/998/1/012018

Mohamed, M. M. and El-Baky, M. A. A., Air cooling of mini-channel heat sink in electronic devices, *J. Electron. Cooling. Therm. Control.*, 3(2), 49–57(2013). http://dx.doi.org/10.4236/jectc.2013.32007

Moldoveanu, G. M., Huminic, G., Minea, A. A. and Huminic, A., Experimental study on thermal conductivity of stabilized Al_2O_3 and SiO_2 nanofluids and their hybrid, *Int. J. Heat. Mass. Transf.*, 127, 450–457(2018). https://doi.org/10.1016/j.ijheatmasstransfer.2018.07.024

Mukherjee, S., Wcislik, S., Khadanga, V. and Mishra, P. C., Influence of nanofluids on the thermal performance and entropy generation of varied geometry microchannel heat sink, *Case. Stud. Therm. Eng.*, 49, 103241(2023). https://doi.org/10.1016/j.csite.2023.103241

Nguyen, C. T., Roy, G., Gauthier, C. and Galanis, N., Heat transfer enhancement using Al_2O_3-water nanofluids for an electronic liquid cooling system, *Appl. Therm. Eng.*, 27(8-9), 1501–1506(2007). https://doi.org/10.1016/j.applthermaleng.2006.09.028

Patel, A. K., Rajput, S. P. S., Kumar, R., Abhishek, S., Singh, A. P., Sharma, M. K., Parveen, G. and Piyush, S., Design and heat transfer performance analysis of mini-channel heat sink with water, EG and EG20 based nanofluids-computational approach, *Int. J. Interact. Des. Manuf.*, 18(4), 2119–2130(2024). https://doi.org/10.1007/s12008-022-00951-9

Peng, X. F. and Peterson, G. P., Convective heat transfer and flow friction for water flow in microchannel structures, *Int. J. Heat. Mass. Transf.*, 39(12), 2599–2608(1996). https://doi.org/10.1016/0017-9310(95)00327-4

Qu, W. and Mudawar, I., Experimental and numerical study of pressure drop and heat transfer in a single-phase micro-channel heat sink, *Int. J. Heat. Mass. Transfer.*, 45(12), 2459–2565(2022). https://doi.org/10.1016/S0017-9310(01)00337-4

Ranjbar, G. S. E., Hosseini, A. A. and Javad, S. M., Cooling performance analysis of water-cooled heat sinks with circular and rectangular minichannels using finite volume method, *Iran. J. Chem. Eng. Res.*, 37(2), 231–239(2018). https://doi.org/10.30492/ijcce.2018.26848

Saadoon, Z. H., Ali, F. H., Hamzah, H. K. Abed, A. M. and Hatami, M., Improving the performance of mini-channel heat sink by using wavy channel and different types of nanofluids, *Sci. Rep.*, 12(1), 9402(2022). https://doi.org/10.1038/s41598-022-13519-0

Selvakumar, P. and Suresh, S., Convective performance of CuO/water nanofluid in an electronic heat sink, *Exp. Therm. Fluid. Sci.*, 40, 57–63(2012). https://doi.org/10.1016/j.expthermflusci.2012.01.033

Seyf, H. R. and Mohammadian, S. K., Thermal and hydraulic performance of counterflow microchannel heat exchangers with and without nanofluids, *J. Heat. Transf.*, 133(8), 081801(2011). https://doi.org/10.1115/1.4003553

Sheik, M. A., Beemkumar, N., Gupta, A., Gill, A., Devarajan, Y., Jayabal, R. and Leo, G. M. L., Study the effect of silicon nanofluid on the heat transfer enhancement of triangular-shaped open microchannel heat sinks, *Silicon.*, 16(1), 277–293(2024). https://doi.org/10.1007/s12633-023-02663-5

Sidik, N. A. C., Convective heat transfer and flow enhancement using nanofluids in divergent-convergent minichannel heatsink, *AIP. Conf. Proc.*, 2689, 030012(2023). https://doi.org/10.1063/5.0117544

Sriharan, G., Harikrishnan, S. and Ali, H. M., Enhanced heat transfer characteristics of the mini hexagonal tube heat sink using hybrid nanofluids, *Nanotechnol.*, 33(47), 475403(2022). https://doi.org/10.1088/1361-6528/ac8995

Sundar, L. S., Irurueta, G. O., Ramana, E. V., Singh, M. K. and Sousa, A. C. M., Thermal conductivity and viscosity of hybrid nanofluids prepared with magnetic nanodiamond-cobalt oxide (ND-Co_3O_4) nanocomposite, *Case. Stud. Therm. Eng.*, 7, 66–77(2016a). https://doi.org/10.1016/j.csite.2016.03.001

Sundar, L. S., Ramana, E. V., Graça, M. P. F., Singh, M. K. and Sousa, A. C. M., Nanodiamond-Fe_3O_4 nanofluids: Preparation and measurement of viscosity, electrical and thermal conductivities, I*nt. Commun.. Heat. Mass. Transf.*, 73, 62–74(2016b). https://doi.org/10.1016/j.icheatmasstransfer.2016.02.013

Sundar, L. S., Singh, M. K. and Sousa, A. C. M., Enhanced heat transfer and friction factor of MWCNT–Fe_3O_4/water hybrid nanofluids, *Int. Commun. Heat. Mass. Transf.*, 52, 73–83(2004). https://doi.org/10.1016/j.icheatmasstransfer.2014.01.012

Thrush, S. J., Comfort, A. S., Dusenbury, J. S., Xiong, Y. and Qu, H., Xue, H., David, J. S., Gary, C. B. and Xia, W., Stability, thermal conductivity, viscosity, and tribological characterization of zirconia nanofluids as a function of nanoparticle concentration, *Tribol. Trans.*, 63(1), 68–76(2019). https://doi.org/10.1080/10402004.2019.1660017

Wole-Osho, I., Okonkwo, E. C., Adun, H., Kavaz, D. and Abbasoglu, S., An intelligent approach to predicting the effect of nanoparticle mixture ratio, concentration and temperature on thermal conductivity of hybrid nanofluids, *J. Therm. Anal. Calorimetry.*, 144, 671–688(2021). https://doi.org/10.1007/s10973-020-09594-y

Yıldız, C., Arici, M. and Karabay, H., Comparison of a theoretical and experimental thermal conductivity model on the heat transfer performance of Al_2O_3-SiO_2/water hybrid-nanofluid, *Int. J. Heat. Mass. Transf.*, 140, 598–605(2019). https://doi.org/10.1016/j.ijheatmasstransfer.2019.06.028